

## ATOMIC MODELS OF MECHANICAL TWINNING AND $\langle 110 \rangle$ -REORIENTATIONS IN BCC-CRYSTALS

I. Yu. Litovchenko<sup>1,2</sup> and A. N. Tyumentsev<sup>1,2</sup>

UDC 538.911:539.374.1

*Atomic models of twinning and formation of  $\langle 110 \rangle$ -reorientation bands in bcc-crystals via  $bcc \rightarrow fcc \rightarrow bcc$ -transformations accompanied by a change in the reverse transformation system are proposed. It is shown that  $\{112\}$  deformation twins are formed in the course of these transformations, when the shears and directions of homogeneous deformation of the reverse transformation occur in the crystallographically equivalent directions, making  $60^\circ$  angles with the initial direction (during the forward transformation) and the Kurdjumov–Sachs relations are valid. A fulfillment of the Nishiyama–Wassermann orientation relationships or a change in the type such dependence in the course of the reverse transformations gives rise to reorientation of the crystal lattice of these microbands around the  $\langle 110 \rangle$ -type directions by the angles  $60^\circ$  or  $(60 \pm 5.23)^\circ$ . An important feature of these models is a considerable contribution of homogeneous transformation deformation of the martensitic type into the value of plastic deformation of the twin.*

**Keywords:** deformation mechanisms, nanocrystals, reversible transformations via alternative pathways, mechanical twinning, crystal lattice reorientations.

### INTRODUCTION

Mechanical twinning is one of the principal mechanisms of deformation of nanocrystalline metallic materials with fcc- and bcc-lattices. When the crystallite dimensions are reduced to the nanoscale level, the motion of perfect dislocations becomes energetically unfavorable: it requires very high stresses to activate the dislocation sources, which gives rise to suppression of plastic deformation via slip [1]. The twinning mechanisms in nanocrystals differ from those in coarse-grained materials, in particular from the traditional polar mechanism [2], since its implementation in nanosized grains needs super-high stresses exceeding the theoretical strength of a crystal. In [3, 4], new twinning mechanisms were shown in fcc-nanocrystals – twinning by the  $a/6\langle 112 \rangle$  partial dislocations emitted from the grain boundary or nucleating in the bulk of the grain or by overlapping of the extended stacking faults.

Twinning in nanocrystals is frequently accompanied by phase transformations not typical for coarse-grained materials. In the course of a molecular dynamic (MD) investigation of the mechanisms of deformation of iron nanofibers it was found out that during tensile loading in the  $[110]$  orientation the plastic flow occurs via a  $bcc \rightarrow fcc$  local phase transformation [5]. In model experiments on tensile loading of molybdenum nanocrystals in the  $\langle 111 \rangle$ -orientation, a  $bcc \rightarrow fcc$ -transformation into a metastable fcc-phase was observed, which persists during the transformation only. Upon unloading it transforms into the initial bcc-lattice [6].

Reversible phase transformations taking place during plastic deformation of nanocrystals are at present intensively investigated. An MD-simulation of plastic deformation of a copper crystallite demonstrated  $fcc \rightarrow bcc \rightarrow fcc$ -transformations at the front of the partial Shockley dislocation motion [7]. The formation of twins (along the  $\{112\}$

---

<sup>1</sup>Institute of Strength Physics and Materials Science of the Siberian Branch of the Russian Academy of Sciences, Tomsk, Russia, e-mail: litovchenko@spti.tsu.ru, <sup>2</sup>National Research Tomsk State University, Tomsk, Russia, e-mail: tyuments@phys.tsu.ru. Translated from *Izvestiya Vysshikh Uchebnykh Zavedenii, Fizika*, No. 5, pp. 142–148, May, 2019. Original article submitted February 12, 2019.

planes) in the bcc -lattice via a sequence of forward plus reverse  $\text{bcc} \rightarrow \text{fcc} \rightarrow \text{bcc}$  -transformations has been recently demonstrated in [8] in the course of an MD-simulation of plastic deformation of bcc-iron. It was found out that in the tip the growing twin the crystal lattice of iron is rearranged from the bcc into fcc configuration and then back to its bcc-form. The formation of the  $54.7^\circ \langle 110 \rangle$ -reorientation bands during  $\text{bcc} \rightarrow \text{fcc} \rightarrow \text{bcc}$ -transformations was shown by the methods of high-resolution transmission electron microscopy in an iron-based alloy [9] and during *in situ* deformation in the column of a transmission electron microscope in the vicinity of an opening crack in molybdenum [10]. Transformations of a similar type were revealed by the MD-methods in the course of simulations of plastic deformation of a bcc-iron nanocrystal in the vicinity of an opening crack [11].

In [7, 12–15], atomic models of the deformation twin formation and  $(54.7^\circ, 60^\circ, 65.2^\circ) \langle 110 \rangle$ -reorientation bands by the mechanisms of forward-plus-reverse martensitic transformations were proposed, which involved a possibility of a change in the reverse transformation pathway. This possibility is demonstrated by the use of the atomic model of martensitic transformations [16] based on the concept of cooperative thermal atomic vibrations in the  $\{110\}$  close-packed planes of the bcc-lattice. Within this model, ‘freezing’ of these vibrations in the extreme positions is followed by the homogeneous tensile-compressive deformation of the Bain-strain type. This model describes the  $\text{bcc} \rightarrow \text{fcc}$  and  $\text{bcc} \rightarrow \text{hcp}$  transformations from the same standpoints. The difference in these transitions is associated with the shear-based (in the case of  $\text{bcc} \rightarrow \text{fcc}$  transitions) and the compensation, or reshuffling (in the case of  $\text{bcc} \rightarrow \text{hcp}$  transitions) mechanisms of the above-mentioned cooperative displacements (vibrations).

In [7, 12], using  $\text{fcc} \rightarrow \text{bcc} \rightarrow \text{fcc}$ -transformations of the martensitic type accompanied by a change in the sign of the reverse transformation shear direction, the atomic models of dislocation nucleation and new twinning mechanisms in fcc-crystals were proposed. The atomic models of forward-plus-reverse  $\text{bcc} \rightarrow \text{fcc} \rightarrow \text{bcc}$ -transformations accompanied by a change in the homogeneous deformation directions during the reverse transformation were reported in [13–15] as the new mechanisms of mechanical twinning in the bcc-lattice. These models, in addition to providing a physical argumentation of the new mechanisms of twinning in nanocrystals [7, 12–15], offer an interpretation of the formation of deformation twins, including those along the planes with complex indices ( $\{113\}$ ,  $\{225\}$ , etc.) in TiNi single crystals [13], reorientation bands with a wide range of high-angle  $(49.5, 60, 60 \pm 5.23)^\circ \langle 110 \rangle$ -reorientations in the alloys based on V and Mo–Re [14, 15], and also interpret the phenomenon of super-high technological ductility of these alloys.

The purpose of this work is to construct an atomic model ensuring a possibility of simulating both mechanical twinning and formation of the bands with a wide range of angle of the  $\langle 110 \rangle$ -reorientation ( $54.7^\circ, 60^\circ, 65.2^\circ, \dots$ ) via forward-plus-reverse (by an alternative pathway)  $\text{bcc} \rightarrow \text{fcc} \rightarrow \text{bcc}$ -transformations involving the shear mode of deformation.

## RESULTS AND DISCUSSION

Similar to the approach taken in [7, 12–15], we used the theory of martensitic transformations reported in [16], describing the  $\text{bcc} \leftrightarrow \text{fcc}$ -transformations as a combination of the homogeneous tensile-compressive deformation and the shears in the  $\{110\}$  planes and  $\langle 110 \rangle$  directions of the bcc-lattice. In the fcc-lattice, their corresponding planes and directions are  $\{111\}$  and  $\langle 112 \rangle$ , respectively. The value of twinning shear in a bcc -crystal is in this case a vector sum of the forward and reverse transformations. The strictly reverse transformation with a change in the shear direction and the signs of homogeneous deformation to the opposite ones results in the initial crystal orientation. On the other hand, the shear stresses causing the forward transformation impede the above transformation. It should be added that there could be such reverse transformation schemes which would favor relaxation of shear stresses, both in the case the forward and reverse transformations.

The direction of shear during the reverse transformation occurs under the action of the local stress field, so this transformation is a way to relax the stresses in the course of formation of the deformation twins or the  $(54.7^\circ, 60^\circ, 65.2^\circ, \dots) \langle 110 \rangle$ -reorientation bands. In this case, the intermediate fcc-structure, via which the transformation is realized, is metastable and exists immediately during the deformation in the fields of high local stresses. The occurrence of the reverse transformation via an alternative pathway, e.g., by a change in the shear direction, is preconditioned by the necessity of relaxing the local internal stresses.

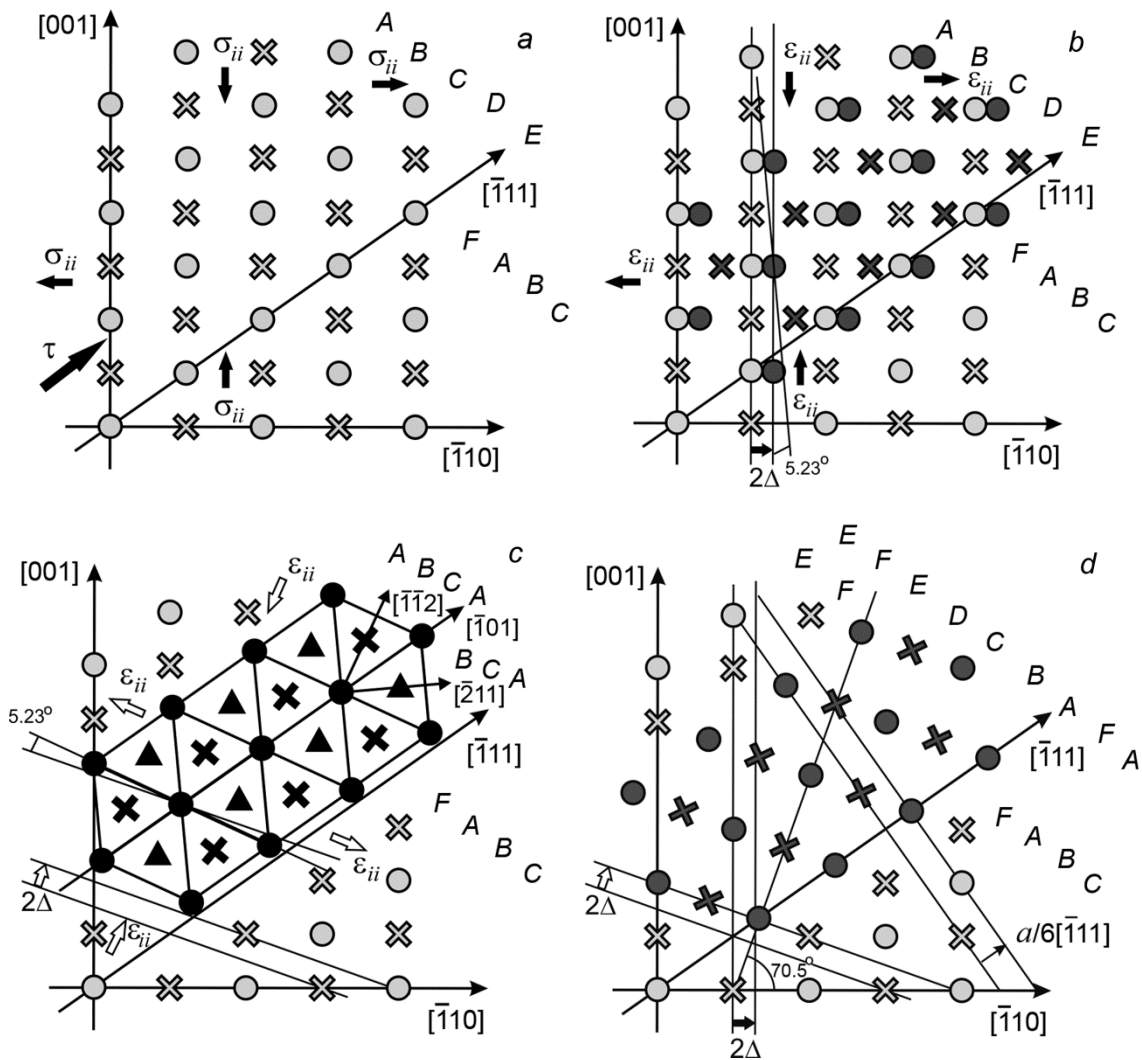


Fig. 1. Formation of nanotwins by the forward-plus-reverse bcc→fcc→bcc-transformation where the (110) plane of the bcc-lattice remains unchanged: *a* – initial bcc-lattice; *b* – after shear deformation via the forward bcc→fcc-transformation, arrows indicate the directions of homogeneous transformation deformation; *c* – fcc-phase interlayer, the directions of shear and homogeneous deformation of the reverse transformation are indicated by arrows; *d* – formation of a twin in the bcc-lattice.

The scheme of a bcc→fcc→bcc -transformation localized in a few planes {112} of the bcc-lattice is presented in Fig. 1. Two planes (110) shown in Fig. 1a correspond to the initial state, the lower-level atoms are indicated by crosses. The {112} planes in this state are packed as follows: ABCDEFABCDEF...

Let us look at a local stress field with a shear component ( $\tau$ ) acting across the (110) plane in the  $[11\bar{1}]$  direction. Given that there are no dislocations in the bcc-crystal and the stresses necessary for their nucleation exceed those needed for a local bcc→fcc-structural transformation, a stress field relaxation becomes possible via this transformation followed by the formation of an fcc-configuration. For this transformation to occur in a local site on several {112} planes of the bcc-lattice, according to [16], a shear strain of  $2\Delta$  is necessary, where  $\Delta$  is the maximum amplitude of the cooperative thermal vibrations (Fig. 1b) in the  $[\bar{1}10]$  direction. This is accompanied by the accommodating atomic displacements and tensile-compressive deformation ( $\epsilon_{ii}$ ), caused by the normal stress components  $\sigma_{ii}$  (Fig. 1b). In this scenario, the shear plane and the shear direction of the forward transformation are (110)

and  $[\bar{1} 10]$ , respectively. When the Kurdjumov-Sachs orientation relationships (KS ORs) are valid between the bcc- and fcc-lattices, it is necessary to add a rotation around the  $[110]$  axis by  $5.23^\circ$  (Fig. 1b) to the shear and homogeneous deformation of the forward bcc→fcc-transformation.

A series of structural rearrangements, taking place under the action of the field stress in a local area of the bcc-lattice, which involve a shear in the  $(110)$  plane along the  $[\bar{1} 10]$  direction, homogeneous tensile-compressive deformation, and a rotation in order to satisfy the ORs, result in the formation of an fcc-structure (Fig. 1c).

In this case, the sequence of atomic packing changes, the bcc  $\{112\}$  planes become  $\{111\}$  planes of an fcc-lattice with the  $ABCABC\dots$  packing of atoms. The fcc-lattice atoms are depicted in Fig. 1c by dark symbols. The concrete values of the tensile-compressive  $\varepsilon_{ii}$  deformation components have not been exactly defined, since the intermediate fcc-phase can exist only during deformation in the fields of high local stresses, and its parameters can essentially depend on the values of the latter. All the plots in Fig. 1 are constructed for the bcc- and fcc-lattice parameters in iron alloys (steels).

The atomic configuration, containing in the local area a non-equilibrium fcc-structure, has a strong thermodynamic stimulus towards a reverse fcc→bcc transformation. The presence of the shear stress component  $\tau$  prevents the reverse transformation from its strictly backward realization with a change in the signs of both the homogeneous and shear deformation modes. The reverse transformation via the alternative pathways becomes possible in the case where the shear strain of the reverse transformation would favor the relaxation of these stresses.

This alternative pathway could be a shear in the same shear plane but in a different direction, specifically in this case, a shear in the  $(111)$  plane of the fcc-lattice in one of the  $\langle 112 \rangle$  directions lying in this plane. In the case of a forward transformation, the  $[\bar{1} 10]$  shear in the bcc-lattice has a corresponding  $[\bar{2} 11]$  shear in the fcc-lattice. In the case of the reverse transformation, the direction of shear in the fcc-lattice is  $[\bar{1} \bar{1} 2]$  (Fig. 1c) and the angle between these directions (indicated by the respective arrows) is  $60^\circ$ . It should be added that the direction of the shear stress component  $\tau$  ( $[11 \bar{1}]$  in the initial bcc-lattice) forms sharp angles  $\approx 30\text{--}35^\circ$  (their specific values are controlled by ORs of the phases) with the shear directions both of the forward and reverse transformations with considerably large ( $\cos(30\text{--}35^\circ) > 0.8$ ) positive values of the Schmidt factor in these directions. The angles between the directions of homogeneous tensile-compressive deformation of the forward and reverse transformations also lie within the range  $\approx 30\text{--}35^\circ$  and depend on the orientation relationships. Thus, a local stress field can favor both the forward and reverse transformation via an alternative pathway.

If the shear deformation ( $2\Delta$ ) of the reverse transformation under the action of stresses  $\tau$  is accompanied by the homogeneous tensile-compressive deformation and a  $5.23^\circ$  rotation about the  $[110]$  axis, a reoriented region in the bcc-lattice is formed around the  $[110]$  direction or the normal to the transformation plane for the K–S OR to be fulfilled (Fig. 1d). This direction remains unchanged in the course of forward-plus-reverse transformations. The shears ( $2\Delta$ ) and homogeneous deformations  $\varepsilon_{ii}$  of the forward and reverse transformations are shown in Fig. 1 by the dark and light arrows, respectively. The total shear in this case represents a shear of the  $a/6[\bar{1} 11]$  partial dislocation by the Burgers vector in the  $(1 \bar{1} 2)$  plane. The total reorientation is determined by the sum of the  $\theta = 60^\circ[110]$  vector, controlled by the choice of the crystallographically equivalent shear directions and the homogeneous deformation of the transformation in the fcc-lattice and two vectors of rotation by  $5.23^\circ[110]$  of the forward and reverse transformations.

If these vectors are summed during the forward and reverse transformations, then the total rotation vector is  $\theta = 70.5^\circ[110]$ , which is equivalent to the twinning in the bcc-lattice across the  $(1 \bar{1} 2)$  plane (Fig. 1d). The initial packing of the  $\{112\}$  planes  $ABCDEFABCDEF\dots$  is transformed into  $ABCDEFEDCBAFABCDEF\dots$  containing an  $FEDCBA$  twin interlayer confined between two stacking faults,  $EFE$  and  $AFA$ , and bounded by the  $a/6\langle 111 \rangle$  partial dislocations. The glide of these dislocations in the  $\{112\}$  planes and  $\langle 111 \rangle$  directions, which is equivalent to the motion of the reorientation front of the forward-plus-reverse transformation, gives rise to a ‘lengthwise’ growth of the twin. The motion of this front in the direction perpendicular to the  $\{112\}$  plane would ensure a ‘breadthways’ growth of the twin.

The versions of the K–S ORs depicted in Fig. 1 are also presented in Table 1. It is evident that during the above-discussed transformation the  $(110)$  plane and the  $[\bar{1} 11]$  direction in the bcc-lattice remain unchanged. In the fcc-lattice, the  $[\bar{1} 01]$  direction changes for the  $[\bar{1} 10]$  crystallographically equivalent direction. The angle between these directions is found to be  $60^\circ$ . The angle between the shear directions of the forward and reverse transformations, given the fulfillment of the K–Z ORs, is  $70.5^\circ$ . Apart from the direction of shear, the directions of homogeneous deformation

TABLE 1. Variants of K–Z ORs of Forward-Plus-Reverse Transformations Ensuring the Formation of a Twin in the bcc-Lattice

Forward transformation	Reverse transformation
$(110)_{\text{bcc}} \parallel (111)_{\text{fcc}}$	$(111)_{\text{fcc}} \parallel (110)_{\text{bcc}}$
$[\bar{1} 11]_{\text{bcc}} \parallel [\bar{1} 01]_{\text{fcc}}$	$[\bar{1} 10]_{\text{fcc}} \parallel [\bar{1} 11]_{\text{bcc}}$

TABLE 2. Variants of K–Z ORs of Forward-Plus-Reverse Transformations Ensuring the Formation of the  $60^\circ\langle 110 \rangle$  Reorientation

Forward transformation	Reverse transformation
$(110)_{\text{bcc}} \parallel (111)_{\text{fcc}}$	$(111)_{\text{fcc}} \parallel (110)_{\text{bcc}}$
$[\bar{1} 10]_{\text{bcc}} \parallel [\bar{2} 11]_{\text{fcc}}$	$[\bar{1} \bar{1} 2]_{\text{fcc}} \parallel [\bar{1} 10]_{\text{bcc}}$

of the reverse transformation also change. A fulfillment of the versions of the K–Z ORs (see Table 1) during the bcc→fcc→bcc-transformations ensures the formation of misorientations with the vectors  $\theta = 70.5^\circ\langle 110 \rangle$ , which are equivalent to twinning in the  $\{112\}$ -type planes of the bcc-lattice.

If during the transformations the Nishiyama–Wassermann orientation relationships (N–W ORs) are fulfilled (Table 2) and, similar to the above-discussed case, the (110) plane of the bcc-lattice remains unchanged, the transformation results in the bcc-crystal reorientation by the  $\theta = 60^\circ[\bar{1} 10]$  vector, which is due to the replacement of the fcc  $[\bar{2} 11]$  direction in the N–W OR by a crystallographically equivalent  $[\bar{1} \bar{1} 2]$  direction lying at the angle  $60^\circ$ , to the first of the above-mentioned directions. The  $[\bar{2} 11]$  shear direction of the forward transformation in the fcc-lattice during the reverse transformation is now replaced for the  $[\bar{1} \bar{1} 2]$  direction. The directions of homogeneous deformation of the reverse transformation, as in the case considered above, are replaced by the crystallographically equivalent ones.

When during the forward-plus-reverse transformations (in the same transformation plane) during the forward transformation the K–Z OR is fulfilled and during the reverse one – N–W OR (or vice versa), the reorientation vectors would be determined by the vector sum  $\theta = 60^\circ\langle 110 \rangle \pm 5.23^\circ\langle 110 \rangle$ , that is  $\theta = 54.7^\circ\langle 110 \rangle$  or  $\theta = 65.2^\circ\langle 110 \rangle$ .

The formation of reorientation regions with the vectors  $\theta = 54.7^\circ\langle 110 \rangle$  was revealed *in situ* by the HRTEM method during the deformation of nanocrystalline Mo in the vicinity of the tip of an opening crack [10], where it was demonstrated that such misorientations are formed in the course of the bcc→fcc→bcc-transformations during which the K–Z ORs are fulfilled in the course of the forward transformation and the N–W ORs – during the reverse one. This reorientation mechanism is also verified by the MD simulations of plastic deformation [10]. Reorientations with similar vectors ( $\theta = 54.7^\circ\langle 110 \rangle$ ) were observed in the bcc-nanocrystals during investigations of a Fe–C alloy after large plastic deformation by high-pressure torsion [9]. The formation of the  $\{112\}$  twins in the course of plastic deformation of a bcc-Fe model crystallite during the bcc→fcc→bcc-transformations was also validated by the MD-methods in [8].

It should be added that the  $54.7^\circ\langle 110 \rangle$ -reorientation bands and  $\{112\}$  deformation twins were observed during plastic deformation of nanocrystals with an fcc-lattice. This could be due to the high local internal stresses and the suppression of the dislocational mechanisms of deformation in nanocrystalline structural states. Stress relaxation in these conditions becomes possible via the forward-plus-reverse bcc→fcc→bcc-transformations.

It is obvious that in the bcc-lattice two mechanisms of formation of the deformation twins and reorientation bands with a specific set of reorientation angles ( $60, 60 \pm 5.23, 70.5^\circ$ ) around the  $\langle 110 \rangle$ -type direction could be singled out:

1. By the bcc→fcc→bcc-transformations with a change in the directions of the homogeneous transformation deformation [13–15].

2. By the bcc→fcc→bcc-transformation mechanism, in which case during the reverse transformation, in addition to the change in the directions of the homogeneous transformation deformation, the direction of shear of the reverse transformation also changes.

The plastic deformation carriers in the above-discussed transformations are the microvolumes of non-equilibrium martensitic phases; furthermore, an important mode of this deformation is the homogeneous transformation deformation of the Bain type.

In the mechanism of the bcc→fcc→bcc-transformation, this is the only deformation mode. Accordingly, the formation of deformation twins via this transformation is a qualitatively different (compared to the dislocation- or shear-induced twinning or martensitic-transformation mechanisms) type of plastic deformation, whose features are determined by the normal stress-field components rather than by the shear components. As it is shown in [17, 18], the deformation twins observed in the latter case do not possess any definite Habit plane and, as a consequence, any coherent twin boundaries characteristic for conventional twinning.

In the atomic model of twinning by the bcc→fcc→bcc-transformation, In the atomic model of twinning by the bcc→fcc→bcc-transformation, involving a shear mode of deformation, the total shear of the forward-plus-reverse transformation is the shear by the Burgers vector of the  $a/6\langle 111 \rangle$  partial dislocations in the  $\{112\}$  twinning plane. This transformation can therefore give rise to the formation of the deformation twins with coherent twin boundaries.

Which of the above-discussed mechanisms controls mechanical twinning is, to our mind, determined by a large number of factors and deformation conditions. Firstly, it is the geometry of the deforming stresses or the character of the local stressed state in the zones of these transformations. Take for instance the value of normal stresses ( $\sigma_{ii}$ ) reduced to the principal axes of the tensor of homogeneous transformation deformation or the Schmidt factor for the motion of a partial dislocation in the twinning plane, which determine possible occurrence of a variety of deformation modes. Secondly, this is the phase diagram stimulating one or the other type of (bcc→hcp or bcc→fcc) of the forward martensitic transformation. Thirdly, these are the concrete conditions (temperature, degree, rate) of deformation and the features of the structural states formed by the onset of the bcc→hcp→bcc or bcc→fcc→bcc-transformations. For instance, these could be grain or nanograin dimensions, defect density, non-equilibrium grain boundaries, texture peculiarities, etc.

It should also be underlined that the above-mentioned transformations can give rise to the formation of a wide range of reorientation bands with a specific set of angles ( $49.5, 60, 60 \pm 5.23, 70.5$ )° of reorientation around the  $\langle 110 \rangle$ -type directions. The formation of a deformation twin (reorientation vector  $\theta = 70.5^\circ \langle 110 \rangle = 180^\circ \langle 112 \rangle$ ) is but an example of such transformations in the case of the fulfillment of the K–Z ORs during the direct and reverse transformations.

To sum up, it is necessary to note that a comparison of the mechanical twinning mechanisms with the mechanisms of formation of partial dislocations and deformation twins during the fcc→bcc→fcc-transformation in the fcc-lattice proposed in [7, 12] indicates the following distinguishing features of these mechanisms in the bcc- and fcc-crystals. In the fcc-lattice, this mechanism is the shear deformation mode alone, since in contrast to the bcc→hcp→bcc-transformations, the reverse transformation is not accompanied by any changes in the directions of the homogeneous tensile-compressive deformation of the Bain type. For this reason, if in the bcc-crystal a necessary condition of twinning is the availability of high values of the normal applied stresses, in the fcc-lattice the formation of deformation twins is controlled by the shear components of these stresses.

During the formation of deformation twins and partial dislocations in the fcc-crystals, these normal stress components control the processes of transformation of the  $\{111\}$  planes into the  $\{110\}$  planes of cooperative thermal vibrations of the bcc-phase, ensuring a possibility of collective displacements of the atoms of these planes by the Burgers vector of the partial dislocation. The homogeneous deformation of the martensitic type occurs during the deformation only, and the value of plastic deformation inside the twin is controlled by the partial dislocation Burgers-vector shears. In the bcc-lattice under the conditions of the bcc→fcc→bcc-transformation this deformation represents a sum of the shear and homogeneous deformation of the martensitic-type transformation. During the bcc→hcp→bcc-transformations, the homogeneous deformation of transformation is the sole deformation mode.

## SUMMARY

A few atomic models of mechanical twinning and formation of the  $\langle 110 \rangle$ -reorientation bands in the bcc-crystals have been proposed, which are based on the mechanism of the forward-plus-reverse  $\text{bcc} \rightarrow \text{fcc} \rightarrow \text{bcc}$ -transformations accompanied by a change in the directions of shear and homogeneous deformation of the reverse transformation for the crystallographically equivalent ones. It has been shown that the  $\{112\}$  deformation twins are formed during the above transformations in the cases, where the shears and directions of the homogeneous deformation of the reverse transformation occur in the crystallographically equivalent directions forming the angles with the initial (during the forward transformation) equal to  $60^\circ$  and the Kurdjumov–Sachs orientation relationships are satisfied. It should be added that in the twinning plane the partial  $a/6\langle 111 \rangle$  dislocations undergo shears by the Burgers vectors and the twin has a coherent boundary. The fulfillment of the Nishiyama–Wassermann orientation relationships or a change in the type such relationships during the reverse transformation result in reorientation of the crystal lattice of the microbands around the  $\langle 110 \rangle$ -type directions by the angles  $60^\circ$  or  $(60 \pm 5.23)^\circ$ . An important peculiarity of these models is a considerable contribution of the homogeneous deformation of the martensitic-type transformation into the value of the plastic deformation of a twin.

## REFERENCES

1. Y. T. Zhu, X. Z. Liao, and X. L. Wu, *Prog. Mater. Sci.*, **57**, 1–62 (2012).
2. J. P. Hirth and J. Lothe, *Theory of Dislocations*, John Wiley & Sons, Inc. (1982).
3. X. Z. Liao, F. Zhou, E. J. Lavernia, *et al.*, *Appl. Phys. Lett.*, **83**, 5062–5064 (2003).
4. K. S. Kumar, H. Van Swygenhoven, S. Suresh, *et al.*, *Acta Mater.*, **51**, 5743–5774 (2003).
5. Y. Zhang, D. J. Yu, and K. M. Wang, *J. Mater. Sci. Technol.*, **28**, No. 2, 164–168 (2012).
6. Zhang Y., Millett P. C., Tonks M., *et al.*, *Acta Mater.*, **60**, 6421–6428 (2012).
7. A. V. Korchuganov, A. N. Tyumentsev, K. P. Zolnikov, *et al.*, *J. Mater. Sci. Technol.*, **35**, 201–206 (2019).
8. K. P. Zolnikov, A. V. Korchuganov, and D. S. Kryzhevich, *Comput. Mater. Sci.*, **155**, 312–319 (2018).
9. Yu. Ivanisenko, I. MacLaren, X. Sauvage, *et al.*, *Acta Mater.*, **54**, 1659–1669 (2006).
10. S. J. Wang, H. Wang, K. Du, *et al.*, *Nature Commun.*, **5**, 3433 (2014).
11. A. Latapie and D. Farkas, *Modelling Simul. Mater. Sci. Eng.*, **11**, 745–753 (2003).
12. A. N. Tyumentsev, I. Yu. Litovchenko, Yu. P. Pinzhin, *et al.*, *Dokl. Akad. Nauk*, **403**, No. 5, 623–626 (2005).
13. A. N. Tyumentsev, N. S. Surikova, I. Yu. Litovchenko, *et al.*, *Acta Mater.*, **52**, 2067–2074 (2004).
14. A. N. Tyumentsev, Yu. P. Pinzhin, I. A. Ditenberg, *et al.*, *Zh. Fiz. Mezomekh.*, **9**, No. 3, 33–45 (2006).
15. A. N. Tyumentsev, I. A. Ditenberg, A. S. Tsverova, *et al.*, *Problems of Atomic Science and Technology. Thermonuclear Fusion*, **41**, Iss. 4, 48–64 (2018).
16. F. A. Kassan-Ogly, V. E. Naysh, and I. V. Sagardze, *Fiz. Met. Metalloved.*, **65**, No. 3, 481–492 (1988).
17. I. A. Ditenberg, A. N. Tyumentsev, *Russ. Phys. J.*, **53**, No. 7, 706–713 (2010).
18. I. A. Ditenberg, A. N. Tyumentsev, and Ya. V. Shuba, *Russ. Phys. J.*, **53**, No. 8, 809–817 (2010).